Journal of Energetic Materials
Publication details, including instructions for authors and subscription information:
http://www.informaworld.com/smpp/title~content=t713770432

Estimation of the Reactive Flow Model Parameters for an Ammonium Nitrate-Based Emulsion Explosive Using Genetic Algorithms

J. B. Ribeiro[a]; C. Silva[b]; R. Mendes[a]
[a] ADAI—Associação para o Desenvolvimento da Aerodinâmica Industrial, Department of Mechanical Engineering, University of Coimbra, Rua Luís Reis Santos, Pólo II, Coimbra, Portugal [b] CEMUC—Centro de Engenharia Mecânica da Universidade de Coimbra, Department of Mechanical Engineering, University of Coimbra, Rua Luís Reis Santos, Pólo II, Coimbra, Portugal

Online publication date: 15 October 2010

To cite this Article Ribeiro, J. B. , Silva, C. and Mendes, R.(2010) 'Estimation of the Reactive Flow Model Parameters for an Ammonium Nitrate-Based Emulsion Explosive Using Genetic Algorithms', Journal of Energetic Materials, 28: 1, 180 — 204
To link to this Article: DOI: 10.1080/07370652.2010.503673
URL: http://dx.doi.org/10.1080/07370652.2010.503673

Journal of Energetic Materials, 28: 180–204, 2010

ISSN: 0737-0652 print/1545-8822 online
DOI: 10.1080/07370652.2010.503673

Estimation of the Reactive Flow Model Parameters for an Ammonium Nitrate–Based Emulsion Explosive Using Genetic Algorithms

J. B. RIBEIRO,[1] C. SILVA,[2] and R. MENDES[1]

[1]ADAI—Associação para o Desenvolvimento da Aerodinâmica Industrial, Department of Mechanical Engineering, University of Coimbra, Rua Luís Reis Santos, Pólo II, Coimbra, Portugal
[2]CEMUC—Centro de Engenharia Mecânica da Universidade de Coimbra, Department of Mechanical Engineering, University of Coimbra, Rua Luís Reis Santos, Pólo II, Coimbra, Portugal

A real coded genetic algorithm methodology that has been developed for the estimation of the parameters of the reaction rate equation of the Lee-Tarver reactive flow model is described in detail. This methodology allows, in a single optimization procedure, using only one experimental result and, without the need of any starting solution, to seek the 15 parameters of the reaction rate equation that fit the numerical to the experimental results. Mass averaging and the plate-gap model have been used for the determination of the shock data used in the unreacted explosive JWL

Address correspondence to J. B. Ribeiro, ADAI—Associação para o Desenvolvimento da Aerodinâmica Industrial, Department of Mechanical Engineering, University of Coimbra, Rua Luís Reis Santos, Pólo II, 3030-788 Coimbra, Portugal. E-mail: jose.baranda@dem.uc.pt

equation of state (EOS) assessment and the thermochemical code THOR retrieved the data used in the detonation products' JWL EOS assessments. The developed methodology was applied for the estimation of the referred parameters for an ammonium nitrate–based emulsion explosive using poly(methyl methacrylate) (PMMA)-embedded manganin gauge pressure–time data. The obtained parameters allow a reasonably good description of the experimental data and show some peculiarities arising from the intrinsic nature of this kind of composite explosive.

Keywords: ammonium nitrate, emulsion, equation of state, explosives, reactive flow

Introduction

Explosive consolidation is essentially a rigid die-pressing technique in which compaction and bonding are achieved by the propagation of explosive-generated shock waves through a loose material. Compacting and bonding are twin objectives of the explosive consolidation and under ideal conditions the two are achieved simultaneously. Recently, the use of explosive-generated shock wave for powder processing is receiving a renewed attention as an alternative route capable of overcoming the traditional problems of the classical techniques for the processing of nanocrystalline, super-hard, high-Tc superconducting composites, metastable highly alloyed, or amorphous powdered materials [1–8]. Despite the promising advantages over the traditional processing routes, this technique still suffers from some problems that are preventing its widespread use in commercial applications. One of those problems is the frequent inhomogeneity of the consolidated samples, with subcompacted or overcompacted (with cracks) regions [1,2]. The mitigation of these problems demands properly designed compaction arrangements. A cylindrical configuration has the potential to overcome those problems [1]. In that configuration a metallic tube containing the powders is surrounded by an explosive composition that, when detonated, starts off a ring-shaped detonation front advancing in the axial direction. This detonation will drive the container wall inward, originating a shock wave that

proceeds into the powder, leading to densification. In this configuration there are two competing mechanisms operating that, when well balanced, can end up with homogeneous compacted/consolidated samples. Those mechanisms are the shock wave pressure increase due to the cylindrical convergence of the front and the shock wave pressure decrease due to energy dissipation caused by localized heat generation, plastic deformation, and comminution of the powder particles during compaction. Balancing these two mechanisms at a pressure level enough for consolidations is, however, a difficult multiparameter task that depends not only on the powder and explosive properties, and their relative amounts (E/M, mass of explosive over mass of powder to compact per unit of length) but also on the nature and thickness of the material of the powder container.

In this situation, computer simulations are of an inestimable importance because they allow a significant reduction of the experimental tests needed to be performed in order to achieve the optimal configuration parameters. Hydrodynamic numerical simulations are currently being used in the design of weapon systems. However, though for the great majority of the solid materials and of the military explosive compositions the value of the input parameters of the material models and of the equation of sate (EOS) is known, for powdered materials and for nonideal (industrial) explosive compositions, like the ones normally used in the compaction processes, those parameters are often not known [2,6]. Given the wide variety of the explosive compositions that can be used and the wide variety of materials that can be processed by this technique, and knowing the importance of working with reliable input data when referring to numerical simulations, it is clear that a useful assistance of the numerical simulation is dependent on the development of an expedite methodology to assess the referred reliable input data for the explosive and powdered material models and EOS.

One of the ways to accomplish that key point is to use inverse analysis. In this kind of analysis the numerical simulations are used not to describe the system behavior for an unknown situation but to replicate a standard experimental situation, sometimes called a *benchmark*. The unknown in this case is

not the system response, experimentally accessed, but the set of parameters of a certain material model or EOS. Given the complexity of the models normally used to describe the explosive and powder material shock behavior, with up to 15 fitting parameters, other than an empirical approach needs to be followed for this searching process. Because we are usually facing poorly understood, and large, search spaces, metaheuristic approaches are thought to be the best [9].

In this article an optimization methodology that combines a genetic algorithm optimizer and the Hydrosoft International version of the HI-DYNA2D numerical code is described. This methodology is also used to assess the 15 parameters of the reaction rate equation of the Lee-Tarver model [10–13] from a single manganin gauge pressure–time profile, without the need for any starting set of parameters, for an ammonium nitrate (AN)-based emulsion explosive. This model is suitable for situations of shock initiation and detonation wave propagation of solid explosives. It should be used whenever there is a question as to whether the explosive will react, whether there is a finite time required for a shock wave to build up to detonation, and/or whether there is a finite thickness of the chemical reaction zone in a detonation wave, which is the case for the nonideal (industrial) explosives used for compaction/consolidation of powders [14–16]. Beyond the referred reaction rate equation, the Lee-Tarver model also uses two Jones-Wilkins-Lee (JWL) EOSs: one for the reactants and other for the detonation products. In this article the first of those EOSs was assessed using the available shock Hugoniot data, the phases rule, and the Thouvenin/plate-gap model for porous materials; the second was assessed from the isentropic expansion data obtained from thermochemical calculations.

Optimization Methodology

To obtain the 15 parameters of the reaction rate equation of the Lee-Tarver model the optimization methodology proposed in this article, as used by April and coauthors [17] for discrete-event simulations and as depicted in Fig. 1, combines a metaheuristic optimizer and a simulation model. In this approach, the

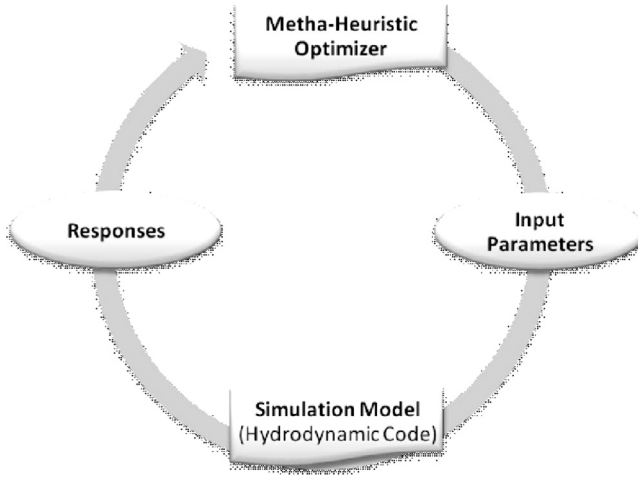

Figure 1. Integrated flowchart of the optimization simulation methodology used in this article.

metaheuristic optimizer chooses a set of values as input parameters of a hydrodynamic code and uses the generated response to make decisions regarding the selection of the next trial solution.

The hydrodynamic code used in this work was the Hydrosoft International (HI) version of the 2D nonlinear explicit finite element (FE) code HI-DYNA2D [14]. This code was used together with a preprocessor module, the HI version of the HI-MAZE [15], for problem definition, which includes mesh generation and specification of the boundary conditions, the materials models, and the material properties. The output of this preprocessor module is a file containing all of the information that defines the problem to be simulated in a format that can be read by the HI-DYNA2D. From all of the information generated by the HI-DYNA2D, the one needed for comparison with the experimental data was assessed using the HI version of the postprocessor HI-ORION [18]. At each HI-DYNA2D run, all the simulation model input data are kept constant except the data referring to the 15 parameters of the reaction rate law. The detailed flow chart of the optimization simulation methodology proposed in this article is presented in Fig. 2.

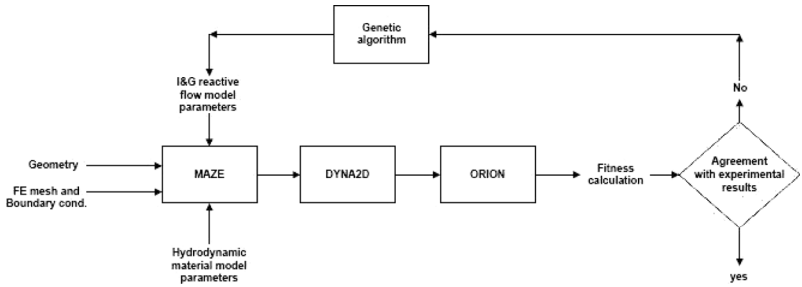

Figure 2. Detailed flowchart of the optimization simulation methodology using the HI-DYNA2D.

Benchmark Experiments

The experimental results used as a benchmark in this work refer to a pressure–time profile from a manganin gauge placed at the end of an 220-mm-long cylindrical explosive charge of AN-based emulsion explosive, confined in a 5-mm-thick polyvinyl chloride (PVC) tube with an internal diameter of 32 mm as shown schematically in Fig. 3. The composition of the emulsion explosive, on a mass basis, was 84% AN, 10% water, and 6% wax. This composition was sensitized with 5% w/w of perlite hollow microspheres. The density of the nonsensitized and sensitized compositions was found, using gravitational methods, to be 1.39 and 1.05 g/cm^3, respectively. The manganin gauge used for this purpose was the J2 M-SS-110FB-048 obtained from Vishay Micro-Measurments (Basing Stoke, Hampshire, UK). This is a grid-like gauge with 48 ohms of resistance, 0.005 mm of thickness, encapsulated in 0.020-mm-thick polymide films. The gauge was placed between two poly(methyl methacrylate) (PMMA) plates with 2 and 8 mm of thickness (front and rear, respectively), using a deaerated low-viscosity epoxy resin and 24 h of curing time. The gauge was connected to a pulsed power supply CK2-50 = 0.05 − 300 obtained from Dynasen (Goleta, CA, USA), whose output, the variation of the electrical tension with the time, was recorded with a 0.001 ms time resolution by a WJ352 oscilloscope (LeCroy, Chestnut Ridge, NY, USA). Voltage data were first converted to resistance through a

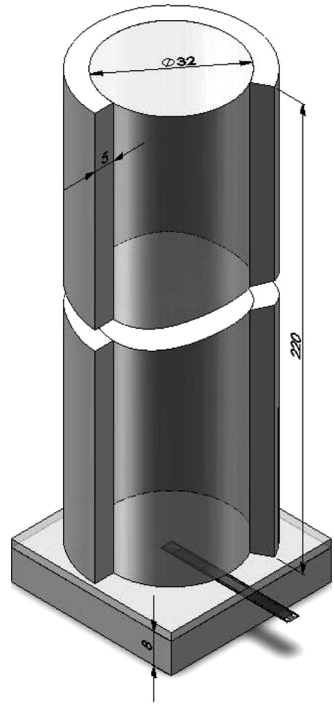

Figure 3. Schematic representation of the experimental setup used to obtain the reference data.

calibration procedure, after which the resistance reduced to pressure using the data from Rosenberg et al. [19]. The obtained result is shown in the graphic of Fig. 4.

Numerical Model

The calculations were performed for an axisymmetrical configuration considering the model of the experimental setup divided in four parts corresponding to (1) rear and front PMMA plates, (2) emulsion explosive, (3) PVC tube wall, and (4) detonator and booster as shown in Fig. 5. The number of elements per millimeter used in each one of these parts was, respectively, two and four for the radial and axial directions in part 1 and one and two for the other parts. The PMMA plates and the PVC wall

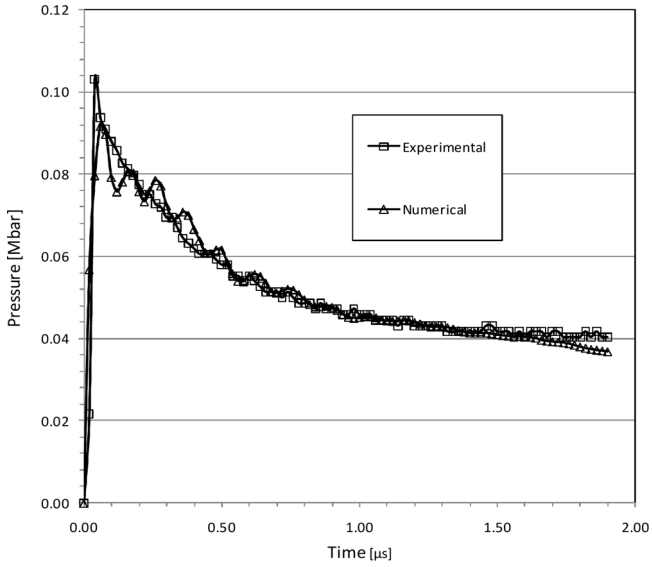

Figure 4. Experimentally (obtained with the setup shown schematically in Fig. 3) and numerically determined pressure–time profiles for a 1.05 g/cm^3 density ammonium nitrate–based emulsion explosive composition.

tube were modeled using the isotropic elastic–plastic hydrodynamic material model coupled with the Grüneisen EOS. For this particular work the shock behavior of PVC was assumed similar to that of PMMA. The values of the parameters of the material model and of the EOS used for this material were the ones available on the HI-DYNA2D embedded database. The initiation of the emulsion explosive was done through the detonation of a pentaerythritol tetranitrate (PETN) booster charge that was model using the high-explosive burn material model coupled with a JWL EOS for the detonation products and, again, the parameter values available in the code-embedded database.

The detonation process in the emulsion explosive was modeled using the isotropic elastic–plastic hydrodynamic material model coupled with the reactive flow model of shock initiation and detonation of heterogeneous solid explosives, or the Lee-Tarver model [11–14]. This model uses two JWL EOSs: one for the

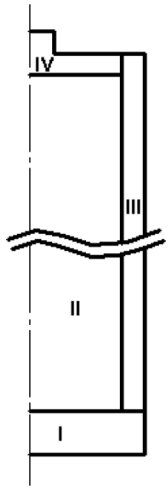

Figure 5. Schematic representation of the model's parts used in the numerical simulations.

unreacted explosive and other for the reaction products, which, in its temperature-dependent form, is shown in Eq. (1):

$$p = A \cdot e^{-R_1 \cdot V} + B \cdot e^{-R_2 \cdot V} + w \cdot C_v \cdot T/V, \tag{1}$$

where P is the pressure, V is the relative volume, T is the temperature, w is the Grüneisen coefficient, C_v is the average heat capacity, and A, B, R_1, and R_2 are constants. As the chemical reaction converts the unreacted explosive to the reaction products, those equations will be used to calculate the pressure in the mixture. This mixture is defined by the fraction of explosive reacted F, where $F = 0$ for no reaction (all explosive) and $F = 1$ for complete reaction (all products). The reaction rate equation for the conversion of the explosive to products is shown as Eq. (2):

$$dF/dt = \underbrace{I \cdot (1-F)^b \cdot \left(\rho/\rho_0 - 1 - a\right)^x}_{0<F<F_{ig\,\max}} + \underbrace{G_1 \cdot (1-F)^c \cdot F^d \cdot P^y}_{0<F<F_{G1\,\max}} + \underbrace{G_2 \cdot (1-F)^e \cdot F^g \cdot P^z}_{F_{G2\,\min}<F<1}, \tag{2}$$

where I, b, a, x, $F_{ig\,\max}$, G_1, c, d, y, $F_{G1\max}$, G_2, e, g, z, and $F_{G2\min}$ are constants.

JWL of the Reactants

The parameters of the JWL EOS of the reactants was assessed by firstly determining the shock Hugoniot of the nonsensitized emulsion composition, including 5% of solid (nonporous) perlite, by mass averaging the parameters of the linear U_s–U_p relation of each one of its components. The values of C_0 and S_1 used for each of the components of this virtual nonporous emulsion are shown in Table 1. It should be noticed that, due to the absence of data in the literature, the perlite of the sensitizing agent was taken as glass and the wax as fuel oil.

Once determined, the mass-averaged values of C_0 and S_1 of the virtual nonporous emulsion, the shock Hugoniot of the porous emulsion was evaluated using the model first introduced by Thouvenin [20] and after slight modification by Hofmann et al. [21]: the plate-gap model. This model considers the porous material as a sequence of plates and gaps in such a manner that the density of this system is equal to the density of the porous solid that is being modeled. The shock propagation in the porous material in this model is assumed to occur as a sequence of plate impacts. The model has already been shown to give good results in the description of the shock data of syntactic foams, a

Table 1
Composition and shock properties of the ammonium nitrated based emulsion explosive studied in this article

	% w/w	C_0 (m/s)	S_1	Reference
Ammonium nitrate	0.798	1,800	1.8	[37]
Water	0.095	1,545	1.8227	[38]
Wax (fuel oil)	0.057	1,786	1.7858	[16]
Perlite (glass)	0.05	3,780	0.8965	[38]
Emulsion	1	1,874	1.7562	

composite material resulting from the mixture of hollow glass microspheres and a polymeric binder [22,23]. The results of the application of the model to the porous emulsion are shown in Fig. 6.

Finally, the coefficients of the JWL EOS (Eq. (1)), except the $w.C_v$ product that, based on the typical values of C_v and w for composite propellants used by other authors [24] was fixed as 1.00E-5 Mbar/K, were determined fitting the equation to the plate-gap model results using the data analysis software Graphis Kylebank Software (Ayrshire, UK). In this process the value of the temperature was kept constant and equal to 298 K.

The obtained parameters are shown in Table 2 and the plot of Eq. (1) with those parameters is shown in Fig. 6.

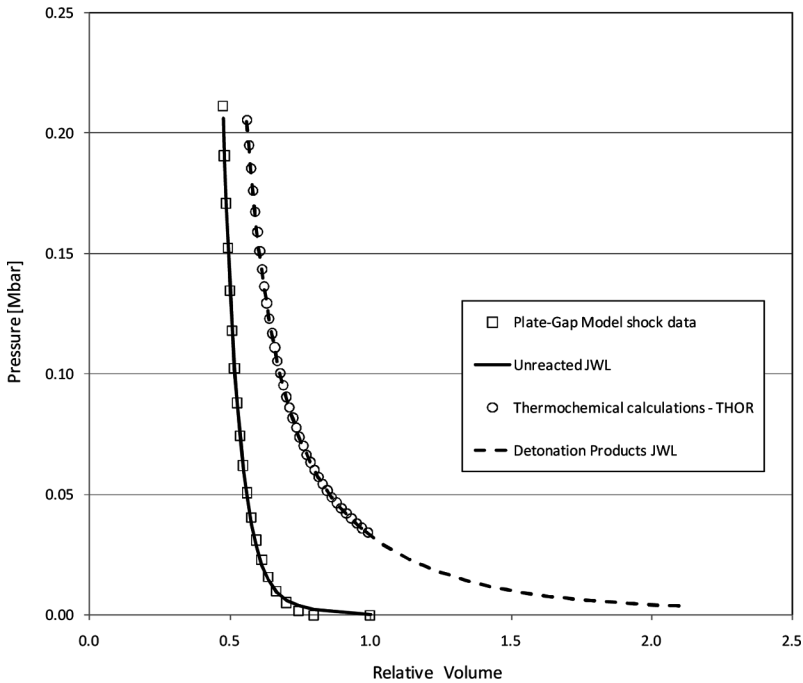

Figure 6. Emulsion explosive unreacted shock data (plate-gap model), detonation product's isentrope (thermochemical code THOR), and associated JWL curves.

Table 2
Unreacted and reacted JWL EOS parameters used in the numeric simulations

	Unreacted	Detonation products
A (Mbar)	1,028	75.39
R_1	17.88	11.95
B (Mbar)	−0.000629	0.4718
R_2	−1.542	2.877
$w.C_v$ (Mbar/K)	1.0E-05	3.0E-06

Detonation Products JWL

In a similar procedure as for the reactants, the parameters of the JWL EOS of the detonation products was assessed by fitting the equation to calculated data. The data used for that purpose were obtained using the thermochemical code THOR and refer to the isentropic expansion (pressure and temperature versus relative volume data) of the detonation products [25]. The calculations were performed for the sensitized porous emulsion composition using as hollow perlite microsphere simulant and artificial low-density ($\rho = 170\,\mathrm{g/cm^3}$, which corresponds to the density of a hollow microsphere with 1 μm of wall thickness and 75 μm of diameter) perlite in the reactants that appear in the detonation products as full dense solid, similar to glass, with a density of 2.65 g/cm^3 and with the following shock parameters: $C_0 = 3.35\,\mathrm{mm/\mu s}$ and $S_1 = 1.56$. The calculated data are shown in Fig. 6.

As for reactants, and with the same exception ($w.C_v$ based on typical values of C_v and w for detonation products and fixed as 3.0E-6 [12,26]), the coefficients of the detonation product's JWL EOS were determined fitting the equation to the calculations using the data analysis software. In that process, using the T-V data from the calculations, the temperature was expressed as a function of the relative volume V using the following equation:

$$T(V) = \sum_{n=0}^{6} \frac{a_n}{V^n} \tag{3}$$

where a_n is a constant and V^n is the relative volume taken to the n exponent. The parameters obtained using this procedure are shown in Table 2 and the plot of Eq. (1) with those parameters is shown in Fig. 6.

Genetic Algorithm Description

Genetic algorithms (GAs) are stochastic general-purpose search methods that use principles inspired by natural genetic populations to evolve solutions for problems [27,28]. GAs have been considered as one of the most appropriate search methods for problems with large, complex, and poorly understood search spaces [17]. GAs are also recognized for their robustness and their independence from the requirement of a high-quality initial guess. A GA starts with a population of randomly generated chromosomes (solutions), advancing toward better chromosomes by applying genetic operators. By this approach, the GA will explore a large portion of the search space and is unlikely to converge to a local minimum. GAs are even capable of searching for solutions from disjoint feasible domains and of operating on irregular functions and on functions that are not differentiable [29]. Through successive iterations, the chromosomes in the population are rated for their adaptation as solutions and, on the basis of these evaluations, a new population of chromosomes is generated using a selection criterion and genetic operators such as crossover and mutation. To evaluate the quality of a given chromosome, a fitness function that returns a single numerical fitness is used. The fitness is proportional to the utility, or adaptation, of the solution represented by the chromosome.

A detailed description of the GA developed by the authors to obtain the set of parameters of the reaction rate law is given as follows.

Chromosome

Each chromosome must represent, without any ambiguity, a solution to the problem that we intend to solve. In our case, the problem is the numerical simulation using the reactive flow

model, as described in the previous section, of a given experimental detonation event. The objective that we intend to achieve using the GA is a set of 15 parameters of the reaction rate equation that fit, to a certain desired degree, the numerical results to the experimental results. These parameters, as well as the limits of the search space, empirically established based on the physical meaning of each parameter as defined by Lee and Tarver [11], Tarver and Hallquist [12], and Tarver et al. [13] and based on several examples of numerical simulations of detonation processes using the same model, are shown in Table 3.

A solution to our problem will be represented by a chromosome (C) made of 15 genes, each one consisting of a real value, ranging from 0 to 1 (see Eq. (4)).

$$C = (c_1, c_2, c_3, c_4, c_5, c_6, c_7, \ldots, c_{13}, c_{14}, c_{15}); c_i \in [0, 1] \tag{4}$$

The gene c_i will generate the parameter $P(i)$ presented in Table 3, row i, using Eq. (5) to ensure that even for parameters with very wide limits of variations, the relative differences observed for the initial randomly generated genes are kept for the parameter values.

$$P(i) = Min(i) \cdot 10^{\left[Log_{10}\left(Max(i)/Max(i)\right)\times c_i\right]} \tag{5}$$

Chromosome Adaptability Evaluation

The evaluation of the chromosome adaptability, or the ability of a given set of parameters to describe the experimental results, is performed using the fitness function $f(C)$ shown in Eq. (6) for a given chromosome j,

$$f(C_j) = \sum_{k=1}^{n\exp ts} |Xexp(tk) - Xsim(tk)| \tag{6}$$

where *nexpts* is the number of experimental values considered for comparison (in this case, $nexpts = 100$), $Xexp(tk)$ is the experimental value of the shock pressure within the PMMA

Table 3
Allowed limits of variation of the reaction rate equation parameters and obtained optimized values

Parameter	Range		Optimized value
	Min.	Max.	
a	0	0.5	0.002
b	0.1	1	0.673
x	1	300	12.291
G_1 (GPa^{-y}. μs^{-1})	$0.1 \times (100)^{-y}$	$1{,}000 \times (100)^{-y}$	116.502
y	1	3	2.026
c	0.1	1	0.407
d	0.01	1	0.030
G_2 (GPa^{-z}. μs^{-1})	$1 \times (100)^{-z}$	$2{,}000 \times (100)^{-z}$	27.957
e	0.1	1	0.534
g	0.1	1	0.630
z	1	5	3.918
$F_{ig\max}$	0.001	1	0.118
$F_{G1\max}$	0.1	1	0.339
$F_{G2\min}$	0.1	1	0.339
i (μs^{-1})	1	1.0E + 13	821,776

barrier at time tk (see section on benchmark experiments), and $Xsim(tk)$ is the shock pressure within the PMMA barrier obtained by numerical simulation using the reaction rate equation parameters generated by the chromosome (j) being tested. It should be noted that being thus defined, the fitness function is a measurement of the difference between the numerical and experimental results, which according to the objectives of this work, should be minimized.

Optimization Procedure

As is typical for the case of single-objective GAs, the optimization procedure starts with a randomly generated but fitness-ranked population of chromosomes, after which it is

followed by a loop over the course of generations in which, driven by the selection process, an offspring population of new chromosomes is created. For the specific case of the GA developed and used in this work, the main steps are detailed below.

Step 1—GA Initialization. To initialize the GA, 100 chromosomes are randomly generated. This means that the GA will work with a population composed of 100 individuals. The choice of the population size was based on our past experience with GAs. In the future, the performance of the GA will be evaluated for different population sizes.

Step 2—Selection Mechanism. From the previous population, the GA will select two individuals to generate an offspring chromosome. A wide set of selection mechanisms has been described in the literature. A good review of these mechanisms is presented by Herrera and coauthors [9]. The GA described in this article uses the proportional selection mechanism, where the probability of selecting the chromosome $c_j[p_s(C_j)]$ is given by:

$$p_s(C_j) = 1 \Big/ \left(f(C_j) \Big/ \sum_{j=1}^{100} f(C_j) \right) \tag{7}$$

where $f(C_j)$ represents the fitness of chromosome j.

In this way, chromosomes with below average fitness tend to be selected more often to generate offspring than those with above average fitness. It should be noted again that a low fitness value is achieved when the parameters, represented by the chromosome, used by the simulator result in a good correspondence between the experimental and simulated results.

Step 3—Crossover Operation. The crossover operator lets a suitable chosen pair of individuals mate with each other to produce offspring. This operator combines the features of the two parent chromosomes, selected in step 2, to form one offspring. It is expected that two good chromosomes may generate better ones. In the proposed GA, we decided to

implement the extended intermediate crossover [30]. This crossover acts as follows:

If $C_1 = \left(c_1^1, c_2^1, c_3^1, c_4^1, c_5^1, \ldots c_{13}^1, c_{14}^1, c_{15}^1\right)$ and $C_2 = \left(c_1^2, c_2^2, c_3^2, c_4^2, c_5^2, \ldots, c_{13}^2, c_{14}^2, c_{15}^2\right)$ are the two chromosomes that have been selected to apply the crossover operator, then the genes of the offspring are generated according to Eq. (8),

$$o_i = \lambda_i \cdot c_i^1 + (1 - \lambda_i) \cdot c_i^2 \tag{8}$$

where λ_i is a randomly generated value in the interval $[-0.2, 1.2]$. Figure 7 illustrates how two parent chromosomes, C_1 and C_2, generate an offspring chromosome.

Step 4—Mutation. To reduce the losses in diversity and the risk of being caught in a local solution, the chromosome generated in step 3 can be mutated. The mutation operator arbitrarily changes the value of one of the genes of the selected chromosome. In the developed GA, the mutation probability was set to 5%. This means that a chromosome formed in the previous step has a probability of 5% of being mutated. If a chromosome is selected to be mutated, one of its genes is randomly chosen for mutation, and the selected gene will be substituted by a new value randomly generated in the interval [0,1].

Step 5—Population Substitution. Steps 2, 3, and 4 are repeated until 98 offspring are generated. After being formed,

Gene; i	1	2	3	4	5	6	7	...
Min	0	0.1	1	0.1	1	0.1	0.001	...
Max	0.5	1	300	1000	3	1	1	...
C_i^1	0.290	0.844	0.106	0.641	0.725	0.137	0.453	...
C_i^2	0.761	0.403	0.500	0.957	0.522	0.288	0.026	...
$I_{i\,(randomized)}$	0.521	0.504	0.596	1.171	0.048	0.381	0.019	...
O_i	0.516	0.625	0.265	0.587	0.532	0.230	0.034	...
Parameters	0.008	0.422	4.538	22.27	1.794	0.170	0.012	...

Equation 8

Equation 5

Figure 7. Offspring chromosome generation process.

these 98 offspring will be added to the best two individuals from the previous population to form the new generation. This new generation will substitute the previous population and the process is repeated until the stopping criterion is attained. The stopping criterion used in our tests was the generation of 10 consecutive generations without an improvement in the fitness of the best population individual (chromosome).

Obtained Results and Discussion

Despite the absence of experimental shock data of unreacted emulsion explosives to be used for comparison with the data calculated as described in the section on the JWL of reactants, the obtained results presented in Fig. 6 seem reliable. This methodology has already shown good results describing the shock data of polymeric-based syntactic foams, a material that can be considered, from a shock behavior point of view, very similar to the emulsion explosives. The determination of the JWL EOS parameters using the data generated is straightforward and resumes to a simple fitting operation. As far as we know, this is one of the first times that the JWL EOS parameters for unreacted emulsion explosives were accessed. The obtained JWL parameters show non-despicable differences from the ones found for usual high-explosive (HE) [11,12] or composite propellants [24].

The determination of the parameters of the JWL EOS of the detonation products is normally done fitting numerical to experimental results of expansion cylinder tests [26,31–33]. The methodology used in this article avoids the realization of those tests and the numerical to experimental matching procedure. It is simpler and presents results at least as good as those obtained by Hamashima et al. [26] using the traditional approach for the same kind of explosive compositions. However, it should be noted that the isentropic expansion (V-P and V-T) data depend on the ability of the thermochemical code to deal with condensed species in the detonation products.

From a classic detonation theory point of view, P-V data for both the unreacted and reacted (detonation products) emulsion

explosive make sense. Also, the Rayleigh line in Fig. 6 allows the prediction of Chapman-Jouguet (CJ) detonation pressure values in accordance with the values commonly reported for these kinds of explosives and densities.

In reference to the determination of the 15 parameters of the reaction rate equation used by the Lee-Tarver model, for the particular case of the emulsion explosive composition described previously, the GA-based optimization methodology has shown to behave as expected. Without the need for any start solution and defining only the limits of variation for each one of the reaction rate equation parameters, as shown in Table 3, the optimizer was able to, within about 2000 HI-DYNA runs and 86 h, find the parameters, also shown in Table 3, that retrieve the result shown in Fig. 4.

The concordance between the numerical and experimental results can be considered very good for expansion times beyond 0.4 ms. However, for the first 0.4 ms, important details observed in the experimental results, like the initial pressure spike, are not seen in the numerical ones. Moreover, for this initial period, the numerical experiments show an oscillating behavior that does not have a counterpart in the experiments. The reasons for this behavior are believed to be related to the details of the numerical model rather than with the values of the parameters of the two JWL EOSs or of the reaction rate equation used in this case.

Among those details of the numerical model that are believed to determine such behavior are the mesh size and the artificial viscosity, which are known to affect the results in a nonindependent way [34]. Mesh size and artificial viscosity sensitivity analysis needs to be performed in order to define the optimal values for this numerical problem. It was already determined that a simple reduction of the mesh size in the axial direction by a factor of two does not show any significant modifications in the results.

In reference to the values of the reaction rate equation parameters, the main differences when compared to typical high explosives as, for example, LX-17, are those referring to d, the exponent of F in the first growth term, $F_{ig\max}$, $F_{G1\max}$, $F_{G2\min}$,

the limits of applicability of each one of the terms of the rate equation; and z, the exponent of pressure in the last growth term.

In reference to d, such a small value as the one we obtained is not typical. The consequence of such a value is a slightly regressive, inward, burning rate not so different, however, of what is used for some HE in some specific situations [35]. In the Lee-Tarver model's origin, the parameter z accounted for the influence of the pressure on the burning rate. Typically, the pressure exponent for laminar deflagration rates is 1.0; however, for higher pressures and temperatures, there is experimental evidence that the value of this parameter can be doubled. Nevertheless, values of 3 were already used in some situations for this parameter and other authors have stated that the pressure exponent should be considered as a fitting parameter instead of as a constant with a physical background [36]. Thus, the value obtained can be a characteristic of these kinds of explosives. Moreover, it should be said that for the best three solutions we obtained, in the final population the value of parameter z was always around 4.

The values of the parameters that define the limits of applicability of each one of the terms in the rate equation are also considerable different from that normally used in most simulations with HE. The turn-off flag of the ignition term, $F_{ig\max}$, is much bigger than usual, and the turn-off flag of the first growth term, $F_{G1\max}$, and the turn-on flag of the second growth term, $F_{G2\min}$, are significantly smaller than usual for HE. Because the turn-off flag of the ignition term normally takes the value of the initial porosity of the explosive charge, a value of 0.118 is not surprising when the initial porosity of this emulsion composition is about 0.25. In reference to the $F_{G1\max}$ and $F_{G2\min}$ values, and if assuming that the second growth term pretends to simulate a slower (when compared with the first growth term) energy release associated to the completion of the reaction [32], it is surprising to find a value as small as 0.34. Typical values are as high as 0.7 to 0.8 [32,36]. The reason for this is probably related to the high value of the pressure exponent of the second growth term used in this case, which does not allow considering it as just a slow energy release completion reaction term.

Conclusions

A fitting and estimation methodology of model parameters developed by the authors is described in this article. The proposed methodology combines the use of real-coded GA optimization and numerical simulation techniques and, without the need for an initial solution, searches for the set of parameters of a certain material model, or EOS, that minimizes the difference between experimental and numerical results. This methodology, implemented for the specific case of the Lee-Tarver reactive flow model, was used for the estimation of the reaction rate equation parameters of an AN-based emulsion explosive. Mass averaging and the plate-gap model have been used for the determination of the shock data of the sensitized (porous) emulsion and, by a fitting process, the JWL EOS of the unreacted explosive. The JWL EOS of the detonation products was obtained from isentropic expansion data of the thermochemical code THOR assuming the glass of the sensitized agent as inert. The obtained results seem to be in accordance with the general detonation properties known for this kind of explosives.

The experimental results used as a reference for the numerical simulations refer to pressure–time profiles of the shock wave pressure within a PMMA barrier loaded by a 200-mm-long cylindrical charge of the referred explosive.

The best set of the reaction rate equation parameters allows a reasonably good description of the experimental results and it is thought that this description can be improved with a simultaneous mesh size refinement and an artificial viscosity tuning. For some of the reaction rate equation parameters, the differences observed between the values we have obtained and what is typical to use in numerical simulations with HE point to the existence of particular features on the detonation behavior of the emulsion explosives that need to be cross-checked with other sources of data and general knowledge in the area. Given the obtained results, in the near future, the proposed methodology should be able to find the parameters of other material models. Its application for design optimization of explosive compaction systems will also be considered in the very near future.

References

[1] Pruemmer, R. A., T. Balakrishna Bhat, K. Siva Kumar, and K. Hokamoto. 2006. *Explosive Compaction of Powder and Composites*. Enfield, NH: Science Publishers.

[2] Carton, E. P. 1998. *Dynamic Compaction of Ceramics and Composites*. Ph.D. thesis, Technical University of Delft.

[3] Pearson, J. 1983. Introduction to high-energy-rate metal working. In T. Z. Blazynski (ed.), *Explosive Welding, Forming and Compaction*, London: Applied Science Publishers.

[4] Meyers, M. A. 1994. *Dynamic Behavior of Materials*. New York: John Wiley & Sons.

[5] Mamalis, A. G., I. N. Vottea, and D. E. Manolakos. 2001. On the modelling of the compaction mechanism of shock compacted powders. *Journal of Materials Processing Technology*, 108(2): 165–178.

[6] Mamalis, A. G., I. N. Vottea, and D. E. Mandakos. 2006. Development of numerical modelling to simulate the explosive compaction/cladding of YBCO ceramic powders. *Modelling and Simulation in Materials Science and Engineering*, 14(2): 313.

[7] Farinha, A. R., J. B. Ribeiro, R. Mendes, and M. T. Vieira. 2009. Shock activation of [alpha]-alumina from calcinated Al-rich sludge. *Ceramics International*, 35(5): 1897–1904.

[8] Farinha, A. R., R. Mendes, J. Baranda, R. Calinas, and M. T. Vieira. 2009. Behavior of explosive compacted/consolidated of nanometric copper powders. *Journal of Alloys and Compounds*, 483(1–2): 235–238.

[9] Herrera, F., M. Lozano, and J. L. Verdegay. 1998. Tackling real-coded genetic algorithms: Operators and tools for behavioural analysis. *Artificial Intelligence Review*, 12(4): 265–319.

[10] Tarver, C. M. 2005. Ignition and growth modeling of LX-17 hockey puck experiments. *Propellants, Explosives, Pyrotechnics*, 30(2): 109–117.

[11] Lee, E. L. and C. M. Tarver. 1980. Phenomenological model of shock initiation in heterogeneous explosives. *Physics of Fluids*, 23(12): 2362–2372.

[12] Tarver, C. M. and J. O. Hallquist. 1981. Modeling two dimensional shock initiation and detonation wave phenomena in PBX 9404 and LX-17. In *Proceedings of the 7th Symposium*

(International) on Detonation, June 16–19, Annapolis, MD, Naval Surface Weapons Center, NSWC MP 82–334.

[13] Tarver, C. M., J. O. Hallquist, and L. M. Erickson. 1985. Modeling short pulse duration shock initiation of solid explosives. In *Proceedings of the 8th Symposium (International) on Detonation*, July 15–19, Albuquerque, NM, Naval Surface Weapons Center NSWC MP 86–194.

[14] Whirley, R. G., B. E. Engelmann, and J. O. Hallquist. 1992. *DYNA2D—A Nonlinear, Explicit, Two-Dimensional Finite Element Code For Solid Mechanics—User Manual*. CA: Lawrence Livermore National Laboratory—Methods Development Group Mechanical Engineering, Livermore, CA.

[15] Sanford, L. A. and J. O. Hallquist. 1996. *MAZE—An Input Generator for DYNA2D, NIKE2D, TOPAZ2D, and CHEMICAL TOPAZ2D—User Manual*. CA: Lawrence Livermore National Laboratory—Methods Development Group Mechanical Engineering, Livermore, CA.

[16] Mulford, R. N., D. C. Swift, and M. Braithwaite. 2002. Temperature-based reactive flow model for ANFO. In *Proceedings of the Twelfth International Detonation Symposium*, August 11–16, San Diego, CA, Office of Naval Research.

[17] April, J., F. Glover, J. P. Kelly, and M. Laguna. 2003. Practical introduction to simulation optimization. In *Proceedings of the 2003 Winter Simulation Conference*, December 7–10, New Orleans, LA.

[18] Hallquist, J. O. and J. L. Levantin. 1985. *Orion: An Interactive Color Post-Processor for Two Dimensional Finite Element Codes*. CA: Lawrence Livermore National Laboratory, Livermore, CA.

[19] Rosenberg, Z., D. Yaziv, and Y. Partom. 1980. Calibration of foil-like manganin gauges in planar shock wave experiments. *Journal of Applied Physics*, 51(7): 3702.

[20] Thouvenin, J. 1965. Effect of a shock wave on a porous solid. In *Proceedings of the Fourth Symposium (International) on Detonation*, October 12–15, White Oak, MD, U.S. Naval Ordinance Laboratory.

[21] Hofmann, R., D. J. Andrews, and D. E. Maxwell. 1968. Computed shock response of porous aluminum. *Journal of Applied Physics*, 39(10): 4555–4562.

[22] Ribeiro, J., J. Campos, R. Mendes, and I. Plaksin. 2003. Wide range shock wave data for polyester syntactic foams. *Journal de Physique IV France*, 110: 785–790.

[23] Ribeiro, J., R. Mendes, I. Plaksin, J. Campos, and C. Capela. 2009. High-pressure range shock wave data for syntactic foams. In M. D. Furnish, M. Elert, T. P. Russell and C. T. White (eds.), *Shock Compression of Condensed Matter—2009*, Melville, NY: American Institute of Physics.

[24] Tarver, C. M., P. A. Urtiew, and W. C. Tao. 1996. Shock initiation of a heated ammonium perchlorate-based propellant. *Combustion and Flame*, 105(1–2): 123–131.

[25] Duraes, L., J. Campos, and A. Portugal. 1998. Reaction path of energetic materials using THOR code. In S. C. Schmidt, D. P. Dandekar and J. W. Forbes (eds.), *Shock Compression of Condensed Matter—1997*, Woodbury, NY: American Institute of Physics.

[26] Hamashima, H., Y. Kato, and S. Itoh. 2004. Determination of JWL parameters for non-ideal explosive. In M. D. Furnish, Y. M. Gupta, and J. W. Forbes (eds.), *Shock Compression of Condensed Matter—2003*. Melville, NY: American Institute of Physics.

[27] Goldberg, D. E. 1989. *Genetic Algorithms in Search, Optimization, and Machine Learning*. New York: Addison-Wesley.

[28] Holland, J. H. 1975. *Adaptation in Natural and Artificial Systems*. Ann Arbor: University of Michigan Press.

[29] Gosselin, L., M. Tye-Gingras, and F. Mathieu-Potvin. 2009. Review of utilization of genetic algorithms in heat transfer problems. *International Journal of Heat and Mass Transfer*, 52(9–10): 2169–2188.

[30] Mühlenbein, H. and D. Schlierkamp-Voosen. 1993. Predictive models for the breeder genetic algorithm i. continuous parameter optimization. *Evolutionary Computation*, 1(1): 25–49.

[31] Murphy, M. J., R. L. Simpson, P. A. Urtiew, P. C. Souers, F. Garcia, and R. G. Garza. 1996. Reactive flow model development for PBXW-126 using modern nonlinear optimization methods. In S. C. Schmidt and W. C. Tao (eds.), *Shock Compression of Condensed Matter 1995*. Woodbury, NY: American Institute of Physics.

[32] Tarver, C. M., J. W. Kury, and R. D. Breithaupt. 1997. Detonation waves in triaminotrinitrobenzene. *Journal of Applied Physics*, 82(8): 3771–3782.

[33] Davis, L. L. and L. G. Hill. 2002. ANFO cylinder tests. In M. D. Furnish, N. N. Thadhani, and Y. Horie, Melville (eds.), *Shock*

Compression of Condensed Matter—2001. NY: American Institute of Physics.

[34] Zukas, J. A., T. Nicholas, H. F. Swift, L. B. Greszczuk, and D. R. Curran. 1982. *Impact Dynamics*. John Wiley & Sons.

[35] Urtiew, P. A., C. M. Tarver, J. L. Maienschein, and W. C. Tao. 1996. Effect of confinement and thermal cycling on the shock initiation of LX-17. *Combustion and Flame*, 105(1–2): 43–53.

[36] Souers, P. C., R. Garza, and P. Vitello. 2002. Ignition & growth and JWL++ detonation models in coarse zones. *Propellants, Explosives, Pyrotechnics*, 27(2): 62–71.

[37] Courchinoux, R. and P. Lalle. 1994. Unreacted Hugoniot of ammonium nitrate. In S. C. Schmidt, J. W. Shaner, G. A. Samara, and M. Ross (eds.), *High Pressure Science and Technology 1993*. New York: American Institute of Physics.

[38] Marsh, S. P. Ed. 1980. *LASL Shock Hugoniot Data, Los Alamos Series on Dynamic Material Properties*. Berkley: University of California Press.